doi:10.1093/brain/aww145 BRAIN 2016: 139; 2198–2210 | 2198

BRAIN
A JOURNAL OF NEUROLOGY

Functional correlates of the therapeutic and adverse effects evoked by thalamic stimulation for essential tremor

William S. Gibson,[1,*] Hang Joon Jo,[1,*] Paola Testini,[1] Shinho Cho,[1] Joel P. Felmlee,[2] Kirk M. Welker,[2] Bryan T. Klassen,[3] Hoon-Ki Min[1,2,4] and Kendall H. Lee[1,4]

[*]These authors contributed equally to this work.

Deep brain stimulation is an established neurosurgical therapy for movement disorders including essential tremor and Parkinson's disease. While typically highly effective, deep brain stimulation can sometimes yield suboptimal therapeutic benefit and can cause adverse effects. In this study, we tested the hypothesis that intraoperative functional magnetic resonance imaging could be used to detect deep brain stimulation-evoked changes in functional and effective connectivity that would correlate with the therapeutic and adverse effects of stimulation. Ten patients receiving deep brain stimulation of the ventralis intermedius thalamic nucleus for essential tremor underwent functional magnetic resonance imaging during stimulation applied at a series of stimulation localizations, followed by evaluation of deep brain stimulation-evoked therapeutic and adverse effects. Correlations between the therapeutic effectiveness of deep brain stimulation (3 months postoperatively) and deep brain stimulation-evoked changes in functional and effective connectivity were assessed using region of interest-based correlation analysis and dynamic causal modelling, respectively. Further, we investigated whether brain regions might exist in which activation resulting from deep brain stimulation might correlate with the presence of paraesthesias, the most common deep brain stimulation-evoked adverse effect. Thalamic deep brain stimulation resulted in activation within established nodes of the tremor circuit: sensorimotor cortex, thalamus, contralateral cerebellar cortex and deep cerebellar nuclei (FDR $q < 0.05$). Stimulation-evoked activation in all these regions of interest, as well as activation within the supplementary motor area, brainstem, and inferior frontal gyrus, exhibited significant correlations with the long-term therapeutic effectiveness of deep brain stimulation ($P < 0.05$), with the strongest correlation ($P < 0.001$) observed within the contralateral cerebellum. Dynamic causal modelling revealed a correlation between therapeutic effectiveness and attenuated within-region inhibitory connectivity in cerebellum. Finally, specific subregions of sensorimotor cortex were identified in which deep brain stimulation-evoked activation correlated with the presence of unwanted paraesthesias. These results suggest that thalamic deep brain stimulation in tremor likely exerts its effects through modulation of both olivocerebellar and thalamocortical circuits. In addition, our findings indicate that deep brain stimulation-evoked functional activation maps obtained intraoperatively may contain predictive information pertaining to the therapeutic and adverse effects induced by deep brain stimulation.

1 Department of Neurologic Surgery, Mayo Clinic, Rochester, MN, USA 55905, USA
2 Department of Radiology, Mayo Clinic, Rochester, MN, USA 55905, USA
3 Department of Neurology, Mayo Clinic, Rochester, MN, USA 55905, USA
4 Department of Physiology and Biomedical Engineering, Mayo Clinic, Rochester, MN, 55905, USA

Correspondence to: Kendall H. Lee, M.D., Ph.D.,
Department of Neurologic Surgery and Department of Physiology and Biomedical Engineering;
200 1st Street SW, Rochester, MN 55905,

Received February 29, 2016. Revised April 6, 2016. Accepted May 3, 2016. Advance Access publication June 21, 2016

USA
E-mail: lee.kendall@mayo.edu

Keywords: functional MRI; deep brain stimulation; ventralis intermedius nucleus; thalamus; essential tremor

Abbreviations: BOLD = blood oxygen level-dependent; DBS = deep brain stimulation; FTM = Fahn-Tolosa-Marin (tremor rating scale); SMA = supplementary motor area; VIM = ventralis intermedius thalamic nucleus

Introduction

Deep brain stimulation (DBS) is a well-established therapy for movement disorders including essential tremor, Parkinson's disease, and dystonia (Benabid *et al.* 1991; Lagrange *et al.*, 2002; Vidailhet *et al.*, 2005). Stimulation of the ventralis intermedius thalamic nucleus (VIM) has proven to be particularly effective for patients with essential tremor, for whom DBS can cause reductions in tremor severity that persist for years or even decades following surgery (Rehncrona *et al.*, 2003; Sydow *et al.*, 2003; Baizabal-Carvallo *et al.*, 2014). Essential tremor is a disorder with a strong familial component, characterized primarily by a kinetic tremor predominantly affecting the arms, head, and/or voice that occurs during voluntary movements, including writing, eating, and other daily activities (Louis, 2005). The disease is thought to be driven by pathological oscillations within a tremor-related network involving motor-related frontal cortex [sensorimotor, premotor cortex, and supplementary motor area (SMA)], VIM, inferior olivary nucleus, cerebellar cortex and dentate nucleus (Deuschl *et al.*, 2000; McAuley and Marsden, 2000; Pinto *et al.*, 2003; Schnitzler *et al.*, 2009).

Recent functional MRI studies have unveiled structural and functional alterations throughout the cerebello-thalamo-cortical circuit that support the notion that essential tremor is a disorder of pathological network activity (Buijink *et al.*, 2015; Gallea *et al.*, 2015). As the clinical effects of stimulating VIM are comparable to those that have been achieved by thalamic lesioning, it was originally proposed that DBS exerts its effects through local inhibition (Benazzouz *et al.*, 1995; Boraud *et al.*, 1996; Benazzouz and Hallett, 2000; Dostrovsky *et al.*, 2000), thereby blocking pathological oscillations occurring between cerebellum and motor cortex. However, PET studies (Ceballos-Baumann *et al.*, 2001; Perlmutter *et al.*, 2002; Haslinger *et al.*, 2003) and mathematical models (McIntyre *et al.*, 2004*a*, *b*) have shown that therapeutic VIM DBS results in neural activation within distal nodes of the cerebello-thalamo-cortical circuit, suggesting that DBS may exert its effects through a more complex mechanism involving multiple oscillators within the tremor network. Indeed, studies that have combined functional MRI with DBS have shown that the therapy is able to induce changes in functional and effective connectivity across neural networks (Kahan *et al.*, 2012, 2014; Knight *et al.*, 2015; Gibson *et al.*, 2016) in a manner that is dependent on the applied stimulation parameters (Kim *et al.*, 2013; Paek *et al.*, 2015; Gibson *et al.*, 2016). However, the question of how changes in blood oxygen level-dependent (BOLD) signal induced by thalamic DBS are related to the clinical effects of the therapy has yet to be addressed.

In this study, we applied intraoperative functional MRI during VIM DBS in patients with essential tremor to test the hypothesis that the observed DBS-evoked changes in functional and effective connectivity would yield predictive information about clinical outcomes, thereby providing insights into the therapeutic mechanism. In addition, studying anaesthetized patients afforded us the unprecedented opportunity to systematically study the effects of adverse effect-inducing DBS on brain networks. By varying the location of the active contacts on the DBS lead in each subject during the experiment, we were able to apply stimulation settings that did and did not induce a common unwanted sensory adverse effect (paraesthesia) that can be induced by VIM DBS. Our results provide a missing link between the network-level changes induced by thalamic DBS and both the therapeutic and adverse effects of the therapy, and contradict the notion that thalamic DBS ameliorates tremor merely through local inhibition of the thalamus.

Materials and methods

Patients

Ten patients (eight females; mean age: 69.3 ± 7.9 years) diagnosed with essential tremor underwent bilateral VIM DBS stereotactic surgery. The diagnosis of essential tremor was based on the Movement Disorders Consensus Criteria (Deuschl *et al.*, 1998). All patients were approved for surgery by the Mayo Clinic DBS Committee, which is composed of neurologists, neurosurgeons, psychiatrists, neuropsychologists, speech pathologists, and a biomedical ethicist. In all patients, tremor predominantly affected the bilateral upper extremities, and in some patients tremor also affected the head, jaw, and/or voice (Table 1). This study was approved by the Mayo Clinic Institutional Review Board, and all patients provided written informed consent in accordance with the Declaration of Helsinki.

Operative approach

Each patient was secured within the Leksell^{TM} stereotactic head frame (Elekta) and a 1.5 T structural MRI (General Electric Signa HDx, 16x software) scan was performed prior to implantation using magnetization-prepared rapid acquisition gradient-echo (MP-RAGE) sequence (Gibson *et al.*, 2016). The MRI data were merged with the Schaltenbrand and Wahren human atlas (Schaltenbrand and Wahren,

Table 1 Patient information

Patient #	Age	Sex	Handedness	Other regions affected by ET (in addition to bilateral upper extremities)	Tremor medications at time of surgery	FTM (preoperative)	FTM (3 months postoperative) (% change)	Active DBS lead during FMRI	Unilateral FTM score (preoperative; contralateral to active DBS lead)	Unilateral FTM score (3 months postoperative) (% change)	Studied DBS lead: stimulation parameters at 3 months[a]
1	78	F	Right	Head, voice	Clonazepam	13	6 (−54%)	right	5	3 (−40%)	C+ 2− 60 µs, 130 Hz, 3.0 V
2	54	F	Right	Head, voice, upper trunk	Primidone, propranolol	19	7 (−63%)	right	8	3 (−63%)	1+ 3− 60 µs, 180 Hz, 1.15 V
3	68	F	Left	Head	Primidone, topiramate	33	7 (−79%)	right	15	1 (−93%)	C+ 1− 60 µs, 130 Hz, 1.4 V
4	73	F	Right	Head, voice	None	19	3 (−84%)	right	8	0 (−100%)	C+ 0− 60 µs, 130 Hz, 0.8 V
5	74	F	Right	Jaw	Propranolol, gabapentin	17	6 (−65%)	right	9	3 (−67%)	C+ 3− 60 µs, 130 Hz, 2.0 V
6	57	F	Right	Head	Topiramate	12	2 (−83%)	right	4	2 (−50%)	C+ 2− 60 µs, 130 Hz, 1.6 V
7	61	M	Left	Head	Gabapentin	15	3 (−80%)	left	2	0 (−100%)	C+ 2− 60 µs, 130 Hz, 1.45 V
8	60	F	Right	Voice	Primidone, propranolol	8	4 (−50%)	left	4	2 (−50%)	C+ 2− 60 µs, 130 Hz, 2.1 V
9	62	F	Right	Head, voice	Gabapentin, primidone, propranolol	9	3 (−67%)	right	4	2 (−50%)	C+ 3− 60 µs, 130 Hz, 2.0 V
10	66	M	Right	None	Propranolol	18	3 (−83%)	right	10	1 (−90%)	2+ 3− 60 µs, 130 Hz, 1.9 V

ET = essential tremor; FMRI = functional MRI.
[a]Anode (C = case, or implantable pulse generator), cathode, pulse-width, frequency, amplitude.

1977), and stereotactic coordinates were identified for the VIM. Following microelectrode recording, quadripolar DBS electrodes (3387 Medtronic) were implanted bilaterally under local anaesthesia. Lead placement was confirmed by computed tomography (Sensation 64, Siemens): image resolution: $0.59 \times 0.59 \times 1.00\,mm^3$. *Post hoc* analysis of CT-MR fusion data (Supplementary Fig. 1) confirmed that the mean location and standard deviation of the most ventral DBS contact (contact 0) across our subjects was 15 ± 2.4 mm lateral; 18 ± 2.3 mm posterior; 5 ± 4 mm inferior to the anterior commissure in Montreal Neurological Institute (MNI) stereotactic coordinates. When displayed with reference to a human brain atlas (Eickhoff *et al.*, 2007), the region of thalamus occupied by the 40 DBS contacts studied was centred on motor thalamus (VIM) (Supplementary Fig. 1).

Intraoperative functional MRI: data acquisition

The intraoperative functional MRI experiment was performed during pulse generator implantation surgery, 1 week after the DBS lead implantation surgery (for detailed methods, see Gibson *et al.*, 2016). After general anaesthesia induction, a unilateral DBS lead was externalized under sterile conditions and attached to a custom wire connected to an external pulse generator (DualScreen 3628 Medtronic, Medtronic) outside the sterile field. To minimize the effects of susceptibility artefacts produced by subgaleal connectors, the laterality (right in eight patients, left in two patients) of the connected lead was selected such that it was contralateral to the implantable pulse generator (Gibson *et al.*, 2016). Patients were then moved into the magnet bore and all scans were conducted with patients under general anaesthesia (Gibson *et al.*, 2016). Average head specific absorption rate (SAR) values of <0.1 W/kg were recorded during the functional MRI study in all the patients, and a board-certified MRI physicist with expertise in MRI for patients with implanted electronic devices was present during all the sessions (Gorny *et al.*, 2013). An anesthesia team was also present during all sessions and vital signs were continuously monitored. For all sequences, a manufacturer's standard transmit/receive RF head coil was used (1.5-T quadrature head coil, model 46-28211862; GE Healthcare). The functional MRI was acquired using 2-dimensional gradient echo-echo planar imaging (GE-EPI): repetition time/echo time, 3000/50; flip angle, 90°; field of view, 22×22 cm; matrix, 64×64; slice thickness, 3.5 mm with a 0-mm gap thickness. For each acquisition, 135 volumes (the first five volumes were discarded for scanner equilibration) were acquired using a block paradigm, with five 6-s stimulation periods (two volumes) alternated with six 60-s rest periods (20 volumes), for a total time of 6 min 45 s per run. Each patient underwent four runs of functional MRI in a single session with 2 min of rest between each run. During each run, bipolar DBS was applied at 90 µs, 130 Hz, 3 V, with the following contact configurations applied across the four runs in a counterbalanced order: 3−2+, 2−1+, 1−2+, 0−1+. By convention, contact '0' refers to the most ventrally-located contact on the quadripolar DBS lead, contact '3' is the most dorsally-located. The cathode or current source is denoted by '−', and '+' refers to the passive/return contact. Following functional MRI, patients were returned to the operating room for pulse generator implantation.

Clinical evaluation

All clinical evaluations were supervised by a neurologist with subspecialty training in movement disorders. During the week following pulse generator implantation (1–2 weeks following DBS lead implantation), patients underwent DBS programming and clinical evaluation. The adverse effect evaluations were performed using monopolar settings used during the routine DBS programming protocol at our institution. Unilateral monopolar stimulation at each cathode (0−, 1−, 2−, 3−; 130 Hz 60 μs) was applied and amplitude was increased until patients reported experiencing an adverse effect, or to 3 V in the case that no adverse effects were reported. In three patients, we confirmed that monopolar stimulation at pulse width of 60 μs (i.e. 0− Case + 130 Hz 60 μs) resulted in DBS-evoked paraesthesias at the same stimulation amplitude as bipolar stimulation at 90 μs (i.e. 0− 1+ 130 Hz 90 μs) (data not shown). Following adverse effect evaluation, patients underwent routine clinical DBS stimulator optimization and returned at 1 month and 3 months for subsequent programming visits. Tremor severity was evaluated preoperatively, and at each patient's 3 month programming visit, using a modified version of the Fahn-Tolosa-Marin (FTM) tremor rating scale Part A (Fahn *et al.*, 1993), which is routinely used to evaluate the therapeutic effects of tremor at our institution. Tremor severity contralateral to the DBS lead that was active during functional MRI was calculated as the sum of six subscores from upper and lower extremities contralateral to the active lead: upper extremity at rest, upper extremity during extension, upper extremity during flexion, upper extremity during finger-to-nose task (kinetic tremor), lower extremity at rest, and lower extremity during extension. The long-term clinical effectiveness of each DBS electrode studied in the functional MRI experiment was calculated as the per cent change in contralateral FTM score at 3 months relative to the preoperative value for each subject.

Functional MRI processing

Functional MRI data were preprocessed and analysed using AFNI (Analysis of Functional NeuroImages; http://afni.nimh.nih.gov) software packages (Cox, 1996). Prior to processing, image data from two subjects who received left-sided stimulation were flipped with respect to the mid-sagittal plane in order to generate group activation maps with a consistent (right-sided) stimulation lateralization. The high-resolution T_1 anatomical image was aligned to the fifth volume of the EPI time series by affine registration using a local Pearson correlation cost function (Saad *et al.*, 2009). The first four volumes of the time series were removed to ensure that all remaining volumes in the time-series were at magnetization steady state. Despiking and rigid body registration were used to estimate subject movement during EPI scans and to correct for slice acquisition timing (Cox and Jesmanowicz, 1999). In all subjects, estimated displacement due to head motion was <0.5 mm in any given axis between successive time series volumes. The time series were then spatially transformed to the Talairach N27 brain template (Holmes *et al.*, 1998) via affine transformation matrices estimated by registering T_1-images to the N27 template. The spatially normalized EPI data were intensity scaled, and smoothed by a typical Gaussian blur of 6 mm full-width at half-maximum.

At the individual session level, the general linear model estimated the shape of the haemodynamic response with respect to the timing of stimulation. To account for baseline drift and residual motion artefact, regressors included six motion parameters estimated during coregistration and a third-order baseline drift function. A regressor was created for the above-mentioned blocked stimulation paradigm, and convolved with a gamma-variate haemodynamic response function. Following the general linear model process, 40 beta-coefficient activation maps were obtained for the entire subject group (four contact-wise activation maps for each individual subject). To obtain the stimulation-evoked activation map, a group-level linear mixed-effects model was conducted to adjust for within-subject activation baselines and the age effect (Chen *et al.*, 2014) (Supplementary Fig. 2A).

Correlation between deep brain stimulation-evoked activation and the therapeutic effect

For correlation analysis, we defined regions of interest from the group activation map thresholded at a significance level of false discovery rate (FDR) $q < 0.05$ ($P < 0.002$, $t > 3.41$). Beta coefficients were extracted from individual activation maps, averaged within each region of interest, and Pearson correlations between region of interest-averaged beta values and the per cent change in contralateral FTM scores at 3 months for each subject were calculated. Correlations were also assessed between region of interest-averaged beta values and per cent change in contralateral FTM subscores representing postural tremor (upper extremity extended + upper extremity flexed + lower extremity extended) and upper extremity kinetic tremor, respectively. In addition, individual voxels that exhibited correlations between beta values and per cent change in contralateral FTM scores are reported. For this analysis, Monte Carlo simulation indicated that an initial, voxel-wise threshold of $P < 0.01$ and a minimum cluster size of 654 voxels gave a corrected P-value of 0.01 ($\alpha = 0.01$; two-tailed $P < 0.01$; Pearson $r > 0.403$; cluster size $\geqslant 654$ voxels).

Deep brain stimulation-evoked adverse effect map

Based on the results of clinical evaluation, activation maps were categorized into two groups: stimulation localizations at which patients reported experiencing DBS-evoked paraesthesias at or below 3 V, and those for which patients were paraesthesia-free at and below 3 V. A group-level linear mixed-effects model was conducted to examine between-group differences in response to the adverse effect. The model included the age as a between-subject covariate and contact conditions as within-subject covariates (Supplementary Fig. 2B). Monte Carlo simulation indicated that an initial, voxel-wise threshold of $P < 0.01$ and a minimum cluster size of 654 voxels gave a corrected P-value of 0.01 ($\alpha = 0.01$, $t > 2.92$) for the significance level of the group difference between DBS evoked activations with and without paraesthesias.

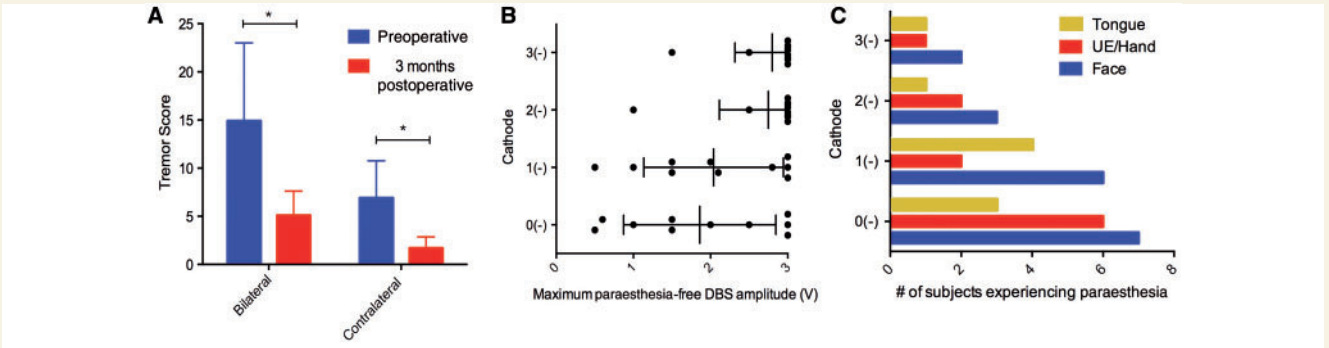

Figure 1 Therapeutic and adverse effects of DBS. (**A**) Bilateral and contralateral FTM scores, before (blue) and 3 months after surgery (red) ($^{*}P < 0.05$, Wilcoxon signed rank). (**B**) Maximum DBS amplitudes tolerated without the presence of adverse effects during clinical evaluation. When no adverse effects were present, stimulator amplitude was increased to 3 V. (**C**) Body areas affected by DBS-evoked paraesthesias, for each stimulation localization (UE = upper extremity).

Dynamic causal modelling

Deterministic, one-state dynamic causal modelling for functional MRI in SPM12 (Wellcome Trust Centre for Neuroimaging, London, UK; http://www.fil.ion.ucl.ac.uk) was used to investigate effective connectivity among established nodes in the tremor-related cerebello-thalamo-cortical loop. BOLD time series data from within a 6-mm sphere centred on the group peak voxel of activation for sensorimotor cortex, thalamus, and contralateral cerebellum (Fig. 2) were included in the analysis. A model representing the established loop, in which VIM thalamus connects reciprocally with motor cortex and contralateral cerebellum, with DBS driving thalamic output, was defined. In one state dynamic causal modelling, connections between brain regions are modelled as excitatory projections, while each region is endowed with inhibitory self-connectivity (Friston *et al.*, 2003). The parameters that represent the strength of between-region (excitatory) and within-region (inhibitory) connections, as well as the driving effect of DBS on the thalamus, are estimated using a posterior density analysis scheme under Gaussian assumptions (Friston *et al.*, 2002). The estimated between- and within-region parameters, given in per second units, or Hertz, describe the degree to which activity in one area is sensitive to changes in activity in another, and has been likened to the concept of electronic gain (Kahan *et al.*, 2012). Inter-regional and within-region connectivity parameters were computed for each subject for each run (40 runs total). Parameter values determined to be significantly different from zero (one sample *t*-test, $P < 0.05$) are reported as 95% confidence intervals (CI). Finally, to determine whether within- or between-region connectivity, as estimated by dynamic causal modelling, correlated with the clinical response, Pearson correlations were assessed between significant between- and with-region connectivity parameters and per cent reduction in contralateral FTM scores.

Results

Therapeutic and adverse effects of deep brain stimulation

At 3 months, patients experienced a significant reduction in tremor severity, both bilaterally ($P = 0.0098$, Wilcoxon signed rank) and contralateral to the DBS lead that was active during the functional MRI experiment ($P = 0.002$, Wilcoxon signed rank) (Fig. 1A). Contralateral reductions in tremor severity ranged from 40 to 100% (median: 65%). Median stimulation parameters for the studied DBS lead at 3 months were 60 µs 130 Hz 1.75 V (Table 1). Of the 40 stimulation localizations that were tested, 23 were associated with stimulation-evoked paraesthesias. These occurred at a median amplitude of 2.0 V (range: 0.6 V to 3 V) (Fig. 1B), and affected the contralateral face (18 settings), contralateral upper extremity and hand (11 settings), and tongue (nine settings) (Fig. 1C). Paraesthesias were most commonly reported at contact 0 (in 9/10 patients), and least commonly reported at contact 3 (in 2/10 patients). Other adverse effects included contraction of facial muscles (two settings) and dysarthria (four settings).

Deep brain stimulation-evoked activation of cerebello-thalamo-cortical circuit correlates with therapeutic effectiveness

The general effect of DBS resulted in three clusters of significant BOLD activation, located in ipsilateral sensorimotor cortex (Fig. 2A), thalamus (Fig. 2B), and contralateral cerebellum (Fig. 2C). Region of interest-level correlation analysis revealed significant positive correlations between therapeutic effectiveness and the extent of BOLD activation in sensorimotor cortex ($P = 0.040$, $r = 0.33$), thalamus ($P = 0.032$, $r = 0.34$), and contralateral cerebellum ($P = 0.0007$, $r = 0.52$) (Fig. 2). Analysis with reference to the Eickhoff-Zilles atlas (Eickhoff *et al.*, 2007) showed that the cerebellar region of interest spanned deep cerebellar nuclei, and lobules V, VI, VIIIa, and IX (Supplementary Fig. 3). Significant voxel-wise correlations were also observed in sensorimotor cortex, thalamus, and contralateral cerebellum, as well as in supplementary motor area, brainstem, and contralateral inferior frontal gyrus (Fig. 3). Finally, a significant region of interest-level correlation between BOLD activation and per

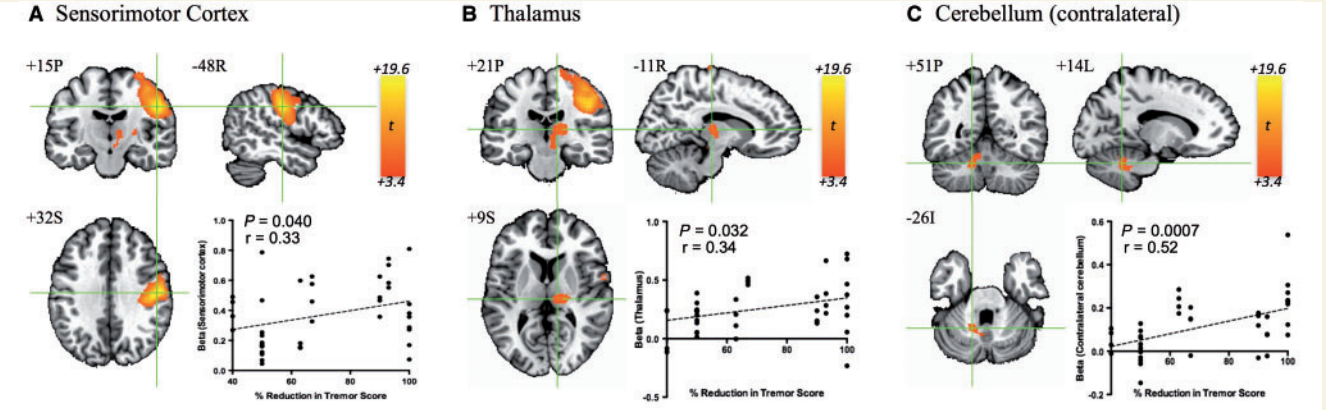

Figure 2 Group activation map evoked by VIM DBS and region of interest-level correlations. DBS resulted in significant BOLD activation (FDR $q < 0.05$; $P < 0.002$, $t > 3.41$) in (**A**) ipsilateral sensorimotor cortex, (**B**) ipsilateral thalamus, and (**C**) contralateral cerebellum. Significant correlations between region of interest-averaged beta values and contralateral per cent reduction in contralateral FTM score were observed ($P < 0.05$) in all three areas.

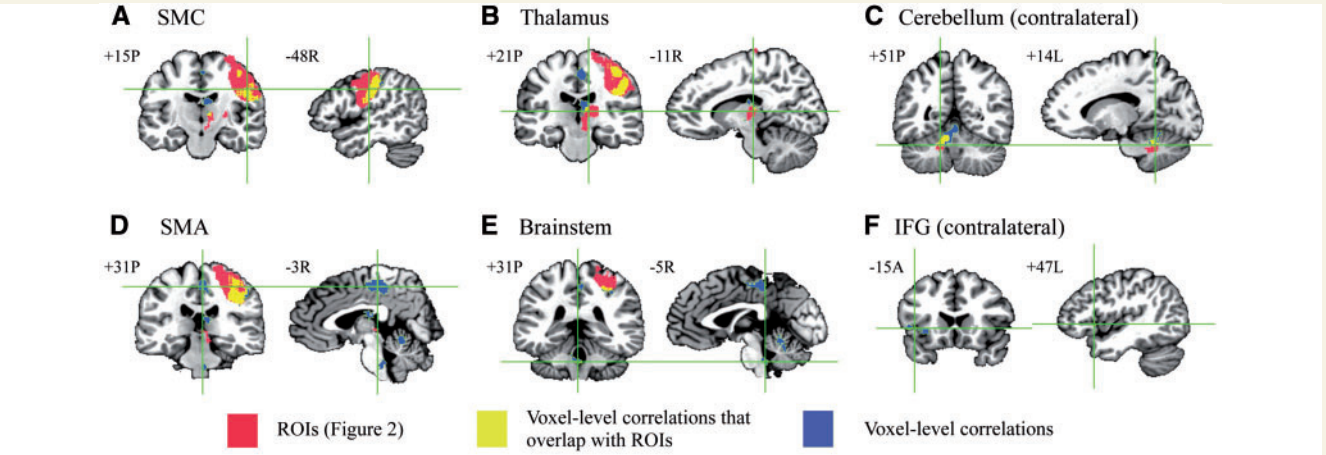

Figure 3 Voxel-level correlations with therapeutic effect. Regions of interest (ROIs) defined in Fig. 2 are shown in red, and regions where voxel-level correlations overlapped with these regions of interest (yellow) and regions in which voxel-level correlations but no significant activation across the group was observed (blue) are shown. Monte Carlo simulation indicated that an initial, voxel-wise threshold of $P < 0.01$ and a minimum cluster size of 654 voxels gave a corrected *P*-value of 0.01 ($\alpha = 0.01$; two-tailed $P < 0.01$; Pearson $r > 0.403$; cluster size $\geqslant 654$ voxels). Region of interest-level correlations in the motor circuit (**A**–**C**) were robust, indicating that the region of interest-level analyses (Fig. 2) are sufficient to capture the major brain–behaviour correlations present in this study. SMC = sensorimotor cortex; IFG = inferior frontal gyrus.

cent change in contralateral FTM subscores related to postural tremor was observed in sensorimotor cortex ($P = 0.017$, $r = 0.39$), while no kinetic tremor-related region of interest-level correlations were observed (Supplementary Fig. 4).

Intrinsic cerebellar connectivity correlates with therapeutic response

DBS exerted an excitatory driving effect (95% CI: 0.06–0.23 Hz, $P = 0.0013$) on the thalamus, which displayed significant excitatory effective connectivity with ipsilateral sensorimotor cortex (95% CI: 0.08–0.24 Hz, $P = 0.0004$) and contralateral cerebellum (95% CI: 0.04–0.12 Hz, $P = 0.0004$) (Fig. 4A and B). In addition, significant inhibitory within-region connectivity was observed in cerebellum (95% CI: −0.033–−0.007 Hz, $P = 0.0027$] (Fig. 4A and B). Attenuated inhibitory within-region connectivity in cerebellum correlated with improved contralateral reduction in tremor severity at 3 months ($r = 0.34$, $P = 0.03$) (Fig. 4C).

Deep brain stimulation-evoked activation of subregions of pre- and postcentral gyri correlate with the presence of paraesthesia

A single region of interest was identified within sensorimotor cortex in which increased BOLD activation was associated with the presence of DBS-evoked paraesthesia (Fig. 5). This region of interest overlapped with a larger region representing the general effect of DBS-evoked

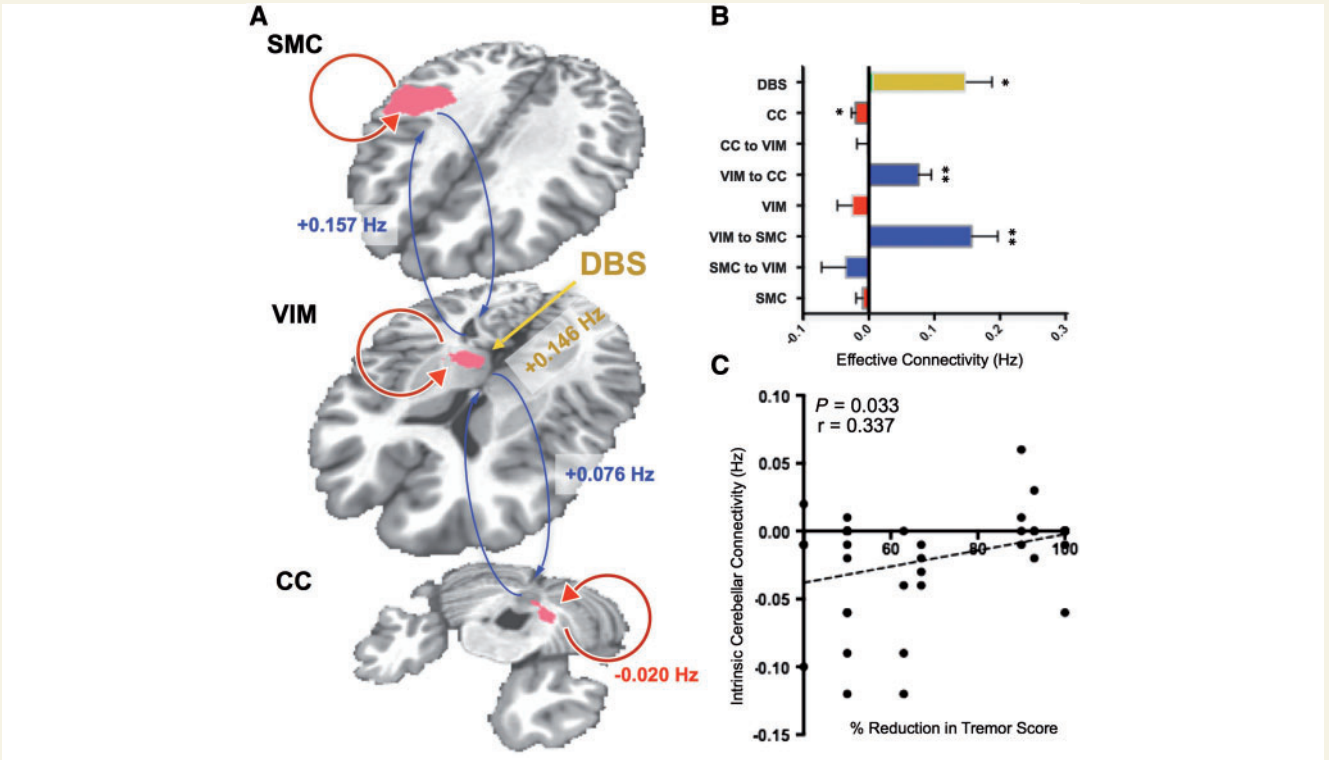

Figure 4 Dynamic causal modelling results. (**A**) Excitatory interregional (blue arrows) and inhibitory within-region (red arrows) connections between sensorimotor cortex (SMC), motor thalamus (VIM), and contralateral cerebellum (CC), and the driving effect of DBS on VIM yellow are shown overlaid on the group DBS-evoked activation map. Connectivity parameters significantly different from zero are shown in **A**, and the estimated values for all connectivity parameters are shown in **B** ($^{*}P < 0.05$, $^{**}P < 0.001$). (**C**) A significant correlation ($P < 0.05$) was observed between within-region inhibitory connectivity in contralateral cerebellum and percent reduction in contralateral tremor score.

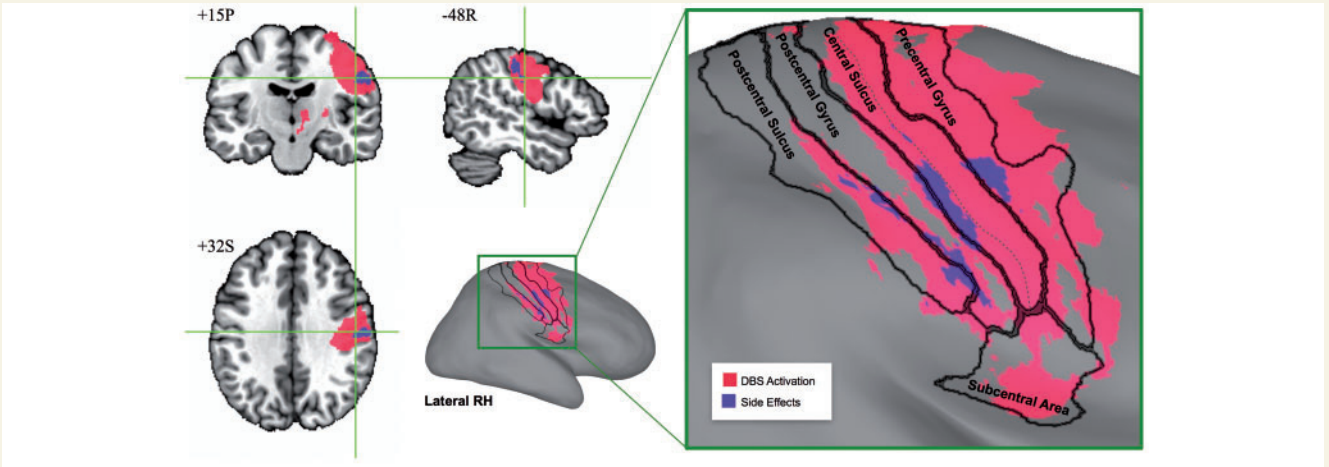

Figure 5 Subregions of sensorimotor cortex associated with the presence of DBS-evoked paraesthesia. These subregions (coloured in purple) are shown with reference to the sensorimotor region of interest corresponding to the general effect of DBS (coloured in pink) overlaid on N27 human brain template (*left*) and its inflated cortical surface (*right*). The area boundaries were mapped from the FreeSurfer cortical parcellation map (Fischl, 2012), and the deepest points of central sulcus are represented by the dashed line.

activation, which spanned pre-, postcentral gyri and sulci, as well as the subcentral area (Fig. 5). The region of interest associated with DBS-evoked paraesthesia included subregions of lateral precentral gyrus, central sulcus, postcentral gyrus, and postcentral sulcus (Fig. 5).

Discussion

Our central finding was that the extent of functional activation in all of the established nodes of the tremor circuit (sensorimotor cortex, SMA, thalamus, cerebellum, and

brainstem) correlated with the long-term therapeutic effectiveness of DBS. According to current theory, essential tremor is likely driven by multiple central oscillatory generators throughout the cerebello-thalamo-cortical circuit that dynamically entrain with one another to produce symptoms of essential tremor (Raethjen *et al.*, 2007; Schnitzler *et al.*, 2009; Raethjen and Deuschl, 2012). The VIM projects to motor and premotor cortices, and is functionally subdivided into a posterior circuit that receives afferents from the cerebellar dentate nucleus (Asanuma *et al.*, 1983), and an anterior circuit that primarily receives afferents from the basal ganglia (Kultas-Ilinsky and Ilinsky, 1991). Therefore, while VIM is situated to modulate all components of the tremor-related cerebello-thalamo-cortical network, our results suggest that network-wide modulation, as opposed to activation of a single brain region or fibre tract, may mediate the therapeutic effects.

The VIM was originally selected as a target for lesioning (Hirai *et al.*, 1983), and later DBS (Benabid *et al.*, 1991), primarily due to its established connectivity with olivocerebellar circuits. The cerebellum has long been thought to play a role in the emergence of essential tremor, due to human neuroimaging (Colebatch, 1990; Jenkins *et al.*, 1993) and animal model electrophysiology data (Llinás and Yarom, 1981, 1986). However, more recent experiments have begun to also implicate motor-related thalamocortical circuits in the mechanism of tremor generation. Studies combining EEG or MEG with EMG recordings have identified tremor-coherent oscillations in motor and premotor cortex (Hellwig *et al.*, 2001; Raethjen *et al.*, 2007; Schnitzler *et al.*, 2009), and coherence and time delay analyses between EEG/MEG recordings and EMG signals have revealed that these oscillations likely reflect cortical output rather than simply sensory feedback (Govindan *et al.*, 2006; Schelter *et al.*, 2009). In addition, single-pulse suprathreshold transcranial magnetic stimulation (TMS) of motor cortex has a known ability to reset tremor (Britton *et al.*, 1993; Pascual-Leone *et al.*, 1994), and continuous TMS can reduce tremor amplitude in patients (Hellriegel *et al.*, 2012). Intraoperative recordings have demonstrated that tremor-related thalamic oscillatory activity is much more likely to occur during movement (Hua and Lenz, 2005), and local field potentials in the thalamus are coherent with electromyography data during muscle contraction but not at rest (Marsden *et al.*, 2000). Together, these results suggest that sensorimotor cortex plays an active role in the production of tremor-related oscillations, rather than simply receiving constant tremor-related olivocerebellar input. Accordingly, our results suggest that DBS brings about its therapeutic effects in part by modulating motor cortex. This hypothesis is also supported by a recent diffusion tensor imaging study, which found that therapeutically effective thalamic DBS preferentially targets thalamic subregions that display enhanced structural connectivity with primary motor cortex (Klein *et al.*, 2012).

While our results implicate thalamocortical afferents in the therapeutic effect, the strongest correlation between DBS-evoked BOLD activation and clinical response was observed in the contralateral cerebellum. Clinical and experimental evidence has consistently implicated cerebellar dysfunction in the pathophysiology of essential tremor. Patients can present with signs of cerebellar dysfunction, including intention tremor (Deuschl and Elble, 2000), balance and gait impairment (Stolze *et al.*, 2001; Kronenbuerger *et al.*, 2009), motor speech impairment (Kronenbuerger *et al.*, 2009), and eye movement abnormalities (Helmchen *et al.*, 2003). Numerous functional neuroimaging studies have reported cerebellar hyperactivity (Colebatch, 1990; Jenkins *et al.*, 1993; Wills *et al.*, 1994, 1995; Bucher *et al.*, 1997; Boecker and Brooks, 1998) and metabolic abnormalities (Louis *et al.*, 2002; Pagan *et al.*, 2003) in essential tremor, and structural changes including atrophy (Quattrone *et al.*, 2008; Cerasa *et al.*, 2009) and reduced fractional anisotropy (Nicoletti *et al.*, 2010). While the origin of these abnormalities remains incompletely understood, Purkinje cells, which provide GABAergic innervation to the dentate nucleus from cerebellar cortex, may play a central role. Post-mortem histological studies have identified axonal and dendritic swelling (Louis *et al.*, 2007, 2011; Yu *et al.*, 2012) and heterotopic displacement in Purkinje cells in essential tremor (Kuo *et al.*, 2011), and some studies have associated reduced Purkinje cell numbers with the disease (Louis *et al.*, 2007; Axelrad *et al.*, 2008; Shill *et al.*, 2008). The correlation reported in this study spanned a region of interest that included deep cerebellar nuclei, as well as cerebellar cortex. The activated region of cerebellar cortex primarily involved a region (lobule VI) displaying connectivity with motor and premotor cortices. Our result therefore suggests that DBS-evoked modulation of motor-related cerebellar outflow, mediated by Purkinje cells, may play an important role in the mechanism of VIM DBS.

In further support of this hypothesis, our effective connectivity analysis revealed a correlation between attenuated within-region inhibitory cerebellar connectivity and the therapeutic effectiveness. Previous reports have suggested that essential tremor is in fact a heterogeneous disease, and degeneration of deep cerebellar nuclei is only seen in a subset of patients (Louis *et al.*, 2006, 2007). Therefore, it is possible that VIM DBS yields greater therapeutic responses (i) in patients in whom Purkinje dysfunction plays a more prominent role in the disease state; or (ii) in patients who received DBS that more effectively targets cerebellar outflow neurons of the dentato-rubro-thalamic tract. In line with the latter hypothesis, efficient targeting of the dentato-rubro-thalamic tract has been correlated with improved outcomes in tremor patients receiving subthalamic nucleus DBS (Groppa *et al.*, 2014). It has been hypothesized that GABAergic deficiency in the dentate nucleus may drive tremor-associated oscillations through disinhibition of cerebellar efferents (Paris-Robidas *et al.*, 2012). We therefore speculate that DBS-evoked activation in deep cerebellar nuclei may be accompanied by an increase in GABAergic tone in the dentate. Indeed, the ability

of DBS to result in GABA release distal to the site of stimulation has been previously demonstrated (Windels *et al.*, 2000, 2003). It has also been shown that activation of thalamic A1 receptors can result in therapeutic effects on tremor, suggesting that the effects of DBS on cerebellar inhibition may also be mediated by adenosine release (Bekar *et al.*, 2008). Further work will be needed to elucidate the precise mechanisms by which VIM DBS modulates tremor-related neurotransmitter concentrations and neural activity in the cerebellum.

Although DBS did not result in significant activation in the brainstem across the subjects studied, a voxel-level correlation between brainstem activation and therapeutic effectiveness was observed (Fig. 3). This result may in part represent DBS-evoked modulation of the inferior olivary nucleus. The neurons of the inferior olivary nucleus send climbing fibre afferents to communicate with Purkinje cells by way of the inferior cerebellar peduncle (Desclin, 1974), which then synapse on GABAergic dentato-olivary projections in the deep cerebellar nuclei (Angaut and Sotelo, 1989). This dentato-olivary loop has been shown to influence cerebellar output during motor tasks (Welsh *et al.*, 1995), and this circuit has been proposed to drive synchrony among Purkinje cells (Hansel, 2009), leading tremor activity to propagate throughout the cerebello-thalamo-cortical circuit. Functional imaging studies have not identified a consistent metabolic alteration in the inferior olivary nucleus in essential tremor patients (Hallett and Dubinsky, 1993; Wills *et al.*, 1994; Bucher *et al.*, 1997). However, ethanol-induced tremor reduction is associated with inferior olivary nucleus activation (Boecker *et al.*, 1996), and the harmaline-induced animal model of essential tremor is known to be mediated by drug-induced bursting activity in the inferior olivary nucleus (Llinás and Yarom, 1981, 1986). The observed correlation provides evidence that the effects of DBS may extend beyond the dentate nucleus to affect the entire olivocerebellar circuit.

A voxel-wise correlation was also observed in the ipsilateral SMA. Several lines of evidence suggest that the SMA may represent another important node in the tremor circuit. Increased grey matter volume in SMA and reduced functional connectivity between SMA and motor cortex has been shown to correlate with tremor severity in patients with essential tremor (Gallea *et al.*, 2015). In addition, tremor-coherent activity has been detected by MEG in premotor areas (Schnitzler *et al.*, 2009), and abnormal activation in SMA has been observed during motor tasks in tremor patients (Neely *et al.*, 2015). It is difficult to speculate regarding the mechanism by which VIM DBS may modulate SMA, since this region displays connectivity with both motor cortex (Dum and Strick, 2005) and cerebellum (Akkal *et al.*, 2007; Bostan *et al.*, 2013), and receives thalamocortical projections from the anterior portion of VIM (Schell and Strick, 1984). Repetitive non-invasive cerebellar stimulation has been shown to alter connectivity between cerebellum and SMA (Popa *et al.*, 2013), potentially implicating modulation of long-range fibres. Our results suggest that thalamic DBS may also modulate these connections.

The only correlation observed outside of the cerebello-thalamo-cortical circuit was located in the contralateral inferior frontal gyrus. As the group activation map mainly represents the effects of right-sided stimulation (8/10 electrodes), this brain region likely represents the left inferior frontal gyrus. Also known as Broca's area (Broca, 1861), it is thought to play a critical role in processing both the phonological aspects and meanings of words (Gabrieli *et al.*, 1998; Indefrey and Levelt, 2000), and therefore is essential for language production and comprehension. Interestingly, high frequency thalamic stimulation for tremor has been shown to cause impairments in verbal fluency, while low frequency stimulation enhances fluency (Pedrosa *et al.*, 2014). Stimulation-evoked fluency impairments have also been observed following subthalamic nucleus DBS in patients with Parkinson's disease, and PET studies in these patients have correlated this effect with decreased activation in prefrontal regions that include Broca's area (Schroeder *et al.*, 2003; Cilia *et al.*, 2007; Kalbe *et al.*, 2009). These findings, coupled with the observation that thalamic DBS induces prefrontal activation in animal models (Paek *et al.*, 2015), suggest that thalamic DBS may exert unexplored effects on prefrontal circuits, particularly those involved in language. While the effect of DBS on verbal fluency was not assessed in this study, our result suggests that prefrontal BOLD correlates of the effects of stimulation on fluency may exist. However, as this correlation (as well as those in SMA in brainstem) was observed in an area that did not exhibit significant activation across the group, and it occurs in a region contralateral to the stimulated nucleus, it must be interpreted with caution.

Our analysis revealed specific subregions of sensorimotor cortex in which DBS-evoked activation correlated with the presence of paraesthesias. While a few case reports have shown differences in functional activation patterns at DBS settings that evoke cognitive and mood-related adverse effects (Schroeder *et al.*, 2003; Stefurak *et al.*, 2003; Cilia *et al.*, 2007; Kalbe *et al.* 2009) the hypothesis that functional MRI could identify cortical regions that mediate sensorimotor adverse effects has not been tested to our knowledge. To investigate this question, we chose the most common adverse effect induced by thalamic DBS, paraesthesia, which results from inappropriate stimulation of neurons in the ventralis caudalis nucleus (Vc), the somatosensory relay nucleus of the thalamus that resides immediately posterior to VIM. The use of intraoperative imaging in anaesthetized patients allowed us to investigate the network-level effects of paraesthesia-inducing DBS without causing patients any discomfort. Our analysis revealed that DBS-evoked paraesthesias were associated with increased activation in a region of the lateral sensorimotor cortex that spanned precentral gyrus, central sulcus, and postcentral sulcus (Fig. 5). This result is supported by human intraoperative cortical mapping experiments,

which have shown that both sensory and motor responses can be elicited by stimulation on either side of the central sulcus (Penfield and Boldrey, 1937; Nii *et al.*, 1996), suggesting that the traditional nomenclature (precentral gyrus = 'motor' and postcentral gyrus = 'sensory') represents an oversimplification. In addition, it is known that cutaneous stimulation can evoke responses in both pre- and postcentral gyri (Fetz *et al.*, 1980). We note that the lateral location of the region of interest associated with paraesthesias corresponds roughly to the face/hand areas of the homunculus, in line with our observation that DBS-evoked paraesthesias were most commonly evoked in the contralateral face, followed by the hand and upper extremity (Fig. 1).

Some limitations and technical points must be considered. First, our DBS-functional MRI experiments were conducted while patients were under general anaesthesia. While this approach allowed us to assess the BOLD effects associated with paraesthesia-inducing stimulation, we note that anaesthesia may influence the DBS-evoked BOLD signal. Patients received both inhaled halogenated ether anaesthetic and intravenous fentanyl during functional MRI acquisition. These drugs have a known ability to depress neuronal activity and metabolism (Ruskin *et al.*, 2013), and can also influence cerebral blood flow and neurovascular coupling (McPherson *et al.*, 1984; Safo *et al.*, 1985; Matta *et al.*, 1999). While the effects of these agents on the BOLD signal remain incompletely characterized, several studies have correlated the presence of anaesthesia with decreases in the magnitude and activation area of stimulus-evoked BOLD responses (Kerssens *et al.*, 2005; Plourde *et al.*, 2006; Aksenov *et al.*, 2015). We previously compared the DBS-evoked BOLD signal in awake versus anaesthetized subjects (Knight *et al.*, 2015), and found that while similar activation areas were observed in both groups, anaesthesia was associated with reduced BOLD signal magnitude. It is therefore possible that the presence of anaesthesia resulted in an underestimation the DBS-evoked BOLD effect. The impact of anaesthesia on the correlations presented here is uncertain, and future studies will be needed to clarify this relationship. Second, the DBS electrode created a susceptibility artefact that reduced the strength of the BOLD signal along the electrode trajectory (Supplementary Fig. 5). Despite this artefact, DBS-evoked BOLD signal at the group level was still observed in the motor thalamus. It is likely, however, that the artefact led to an underestimation of DBS-evoked BOLD in the immediate vicinity of the electrodes, which may have affected the results of our correlation and effective connectivity analyses. We also note that a correlation between BOLD activation and postural, but not kinetic, tremor subscores was observed in sensorimotor cortex (Supplementary Fig. 4). One possible explanation of this result is that preferential targeting of thalamocortical projections may play a more important role in suppression of postural than kinetic tremors in essential tremor. However, we must emphasize that this result is preliminary, as our clinical evaluation of kinetic tremor did not quantitatively differentiate simple kinetic tremor from intention tremor, both of which may be modulated by different mechanisms (Deuschl *et al.*, 2000). In addition, our study may be underpowered to detect correlations between BOLD activation and individual tremor subtypes, and a larger sample size may be necessary to address this question. Finally, the DBS settings used during functional MRI were not identical to those applied chronically. However, this study was designed to test whether BOLD activation patterns obtained intraoperatively, before optimal stimulation parameters had been selected, exhibited correlations with future therapeutic efficacy. We note that this design precludes us from establishing a causal relationship between increased network activation and clinical effects. However, it did allow us to assess whether network activation in response to a standard set of parameters, applied prior to DBS programming, would correlate with improved future therapeutic response. As DBS expands to treat other neurological and psychiatric disorders where obvious clinical signs of efficacy cannot be immediately observed during DBS programming, there will be an increasing need for measures of brain activity, obtained prior to chronic stimulation that could be used to guide this process. While technical hurdles still exist, our results indicate that DBS-evoked BOLD activation patterns may hold untapped potential to fill this unmet need.

Acknowledgements

We would like to thank clinical DBS nurses Janeane Hain, Amy Grassle, and Kelsey McGrane for their assistance with clinical evaluations, as well as Krzysztof Gorny, Ph.D., for his assistance during the experiments.

Funding

This work was supported by The Grainger Foundation and by the National Institutes of Health (R01 NS 70872 awarded to K.H.L.).

Supplementary material

Supplementary material is available at *Brain* online.

References

Akkal D, Dum RP, Strick PL. Supplementary motor area and presupplementary motor area: targets of basal ganglia and cerebellar output. J Neurosci 2007; 27: 10659–73.

Aksenov DP, Li L, Miller MJ, Iordanescu G, Wyrwicz AM. Effects of anesthesia on BOLD signal and neuronal activity in the somatosensory cortex. J Cereb Blood Flow Metab 2015; 35: 1819–26.

Angaut P, Sotelo C. Synaptology of the cerebello-olivary pathway. Double labelling with anterograde axonal tracing and GABA immunocytochemistry in the rat. Brain Res 1989; 479: 361–5.

Asanuma C, Thach WT, Jones EG. Brainstem and spinal projections of the deep cerebellar nuclei in the monkey, with observations on the brainstem projections of the dorsal column nuclei. Brain Res 1983; 286: 299–322.

Axelrad JE, Louis ED, Honig LS. Reduced Purkinje cell number in essential tremor: a postmortem study. Arch Neurol 2008; 65: 101–7.

Baizabal-Carvallo JF, Kagnoff MN, Jimenez-Shahed J, Fekete R, Jankovic J. The safety and efficacy of thalamic deep brain stimulation in essential tremor: 10 years and beyond. J Neurol Neurosurg Psychiatr 2014; 85: 567–72.

Bekar L, Libionka W, Tian GF, Xu Q, Torres A, Wang X, et al. Adenosine is crucial for deep brain stimulation-mediated attenuation of tremor. Nat Med 2008; 14: 75–80.

Benabid AL, Pollak P, Gervason C, Hoffmann D, Gao DM, Hommel M, et al. Long-term suppression of tremor by chronic stimulation of the ventral intermediate thalamic nucleus. Lancet 1991; 337: 403–6.

Benazzouz A, Hallett M. Mechanism of action of deep brain stimulation. Neurology 2000; 55: S13–16.

Benazzouz A, Piallat B, Pollak P, Benabid AL. Responses of substantia nigra pars reticulata and globus pallidus complex to high frequency stimulation of the subthalamic nucleus in rats: electrophysiological data. Neurosci Lett 1995; 189: 77–80.

Boecker H, Brooks DJ. Functional imaging of tremor. Mov Disord 1998; 13: 64–72.

Boecker H, Wills AJ, Ceballos Baumann A, Samuel M, Thompson PD, Findley LJ, et al. The effect of ethanol on alcohol responsive essential tremor: a positron emission tomography study. Ann Neurol 1996; 39: 650–8.

Boraud T, Bezard E, Bioulac B, Gross C. High frequency stimulation of the internal Globus Pallidus (GPi) simultaneously improves parkinsonian symptoms and reduces the firing frequency of GPi neurons in the MPTP-treated monkey. Neurosci Lett 1996; 215: 17–20.

Bostan AC, Dum RP, Strick PL. Cerebellar networks with the cerebral cortex and basal ganglia. Trends Cogn Sci 2013; 17: 241–54.

Britton TC, Thompson PD, Day BL, Rothwell JC, Findley LJ, Marsden CD. Modulation of postural wrist tremors by magnetic stimulation of the motor cortex in patients with Parkinson's disease or essential tremor and in normal subjects mimicking tremor. Ann Neurol 1993; 33: 473–9.

Broca P. Remarques sur le siège de la faculté du language articulé suivies d'une observation d'aphémie (perte de la parole). Bulletin de la Société Anatomique 1861; 6: 330–357.

Bucher SF, Seelos KC, Dodel RC, Reiser M, Oertel WH. Activation mapping in essential tremor with functional magnetic resonance imaging. Ann Neurol 1997; 41: 32–40.

Buijink AWG, van der Stouwe AMM, Broersma M, Sharifi S, Groot PFC, Speelman JD, et al. Motor network disruption in essential tremor: a functional and effective connectivity study. Brain 2015; 138: 2934–47.

Ceballos-Baumann AO, Boecker H, Fogel W, Alesch F, Bartenstein P, Conrad B, et al. Thalamic stimulation for essential tremor activates motor and deactivates vestibular cortex. Neurology 2001; 56: 1347–54.

Cerasa A, Messina D, Nicoletti G, Novellino F, Lanza P, Condino F, et al. Cerebellar atrophy in essential tremor using an automated segmentation method. Am J Neuroradiol 2009; 30: 1240–3.

Chen G, Adleman NE, Saad ZS, Leibenluft E, Cox RW. Applications of multivariate modeling to neuroimaging group analysis: a comprehensive alternative to univariate general linear model. NeuroImage 2014; 99: 571–88.

Cilia R, Siri C, Marotta G, De Gaspari D, Landi A, Mariani CB, et al. Brain networks underlining verbal fluency decline during STN-DBS in Parkinson's disease: an ECD-SPECT study. Parkinsonism Relat Disord 2007; 13: 290–4.

Colebatch J. Preliminary report: activation of the cerebellum in essential tremor. Lancet 1990; 336: 1028–30.

Cox RW. AFNI: software for analysis and visualization of functional magnetic resonance neuroimages. Comput Biomed Res 1996; 29: 162–73.

Cox RW, Jesmanowicz A. Real-time 3D image registration for functional MRI. Magn Reson Med 1999; 42: 1014–18.

Desclin JC. Histological evidence supporting the inferior olive as the major source of cerebellar climbing fibers in the rat. Brain Res 1974; 77: 365–84.

Deuschl G, Bain P, Brin M. Consensus statement of the Movement Disorder Society on Tremor. Ad Hoc Scientific Committee. Mov Disord 1998; 13 Suppl 3: 2–23.

Deuschl G, Elble RJ. The pathophysiology of essential tremor. Neurology 2000; 54: S14–20.

Deuschl G, Wenzelburger R, Löffler K, Raethjen J, Stolze H. Essential tremor and cerebellar dysfunction clinical and kinematic analysis of intention tremor. Brain 2000; 123: 1568–80.

Dostrovsky JO, Levy R, Wu JP, Hutchison WD, Tasker RR, Lozano AM. Microstimulation-induced inhibition of neuronal firing in human globus pallidus. J Neurophysiol 2000; 84: 570–4.

Dum RP, Strick PL. Frontal lobe inputs to the digit representations of the motor areas on the lateral surface of the hemisphere. J Neurosci 2005; 25: 1375–86.

Eickhoff SB, Paus T, Caspers S, Grosbras MH, Evans AC, Zilles K, Amunts K. Assignment of functional activations to probabilistic cytoarchitectonic areas revisited. Neuroimage 2007; 36: 511–21.

Fahn S, Tolosa E, Concepcion M. Clinical rating scale for tremor. In: Jankovic J, Tolosa E, editors. Parkinson's disease and movement disorders. . Baltimore, MD: Williams and Wilkins; 1993. p. 271–80.

Fetz EE, Finocchio DV, Baker MA, Soso MJ. Sensory and motor responses of precentral cortex cells during comparable passive and active joint movements. J Neurophysiol 1980; 43: 1070–89.

Fischl B. FreeSurfer. NeuroImage 2012; 62: 774–81.

Friston KJ. Bayesian estimation of dynamical systems: an Application to fMRI. NeuroImage 2002; 16: 513–30.

Friston KJ, Harrison L, Penny W. Dynamic causal modeling. NeuroImage 2003; 19: 1273–302.

Gabrieli JD, Poldrack RA, Desmond JE. The role of left prefrontal cortex in language and memory. Proc Natl Acad Sci USA 1998; 95: 906–13.

Gallea C, Popa T, García-Lorenzo D, Valabregue R, Legrand A-P, Marais L, et al. Intrinsic signature of essential tremor in the cerebello-frontal network. Brain 2015; 138: 2920–33.

Gibson WS, Cho SH, Abulseoud OA, Gorny KR, Felmlee JP, Welker KM, et al. The impact of mirth-inducing ventral striatal deep brain stimulation on functional and effective connectivity. Cereb Cortex 2016. Advance Access published on March 21, 2016.

Gorny KR, Presti MF, Goerss SJ, Hwang SC, Jang DP, Kim I, et al. Measurements of RF heating during 3.0-T MRI of a pig implanted with deep brain stimulator. Magn Reson Imaging 2013; 31: 783–8.

Govindan RB, Raethjen J, Arning K, Kopper F, Deuschl G. Time delay and partial coherence analyses to identify cortical connectivities. Biol Cybern 2006; 94: 262–75.

Groppa S, Herzog J, Falk D, Riedel C, Deuschl G, Volkmann J. Physiological and anatomical decomposition of subthalamic neurostimulation effects in essential tremor. Brain 2014; 137: 109–21.

Hallett M, Dubinsky RM. Glucose metabolism in the brain of patients with essential tremor. J Neurological Sci 1993; 114: 45–8.

Hansel C. Reading the clock: how purkinje cells decode the phase of olivary oscillations. Neuron 2009; 62: 308–9.

Haslinger B, Boecker H, Büchel C, Vesper J, Tronnier VM, Pfister R, et al. Differential modulation of subcortical target and cortex during deep brain stimulation. NeuroImage 2003; 18: 517–24.

Hellriegel H, Schulz EM, Siebner HR, Deuschl G, Raethjen JH. Continuous theta-burst stimulation of the primary motor cortex in essential tremor. Clin Neurophysiol 2012; 123: 1010–15.

Hellwig B, Häußler S, Schelter B, Lauk M, Guschlbauer B, Timmer J, et al. Tremor-correlated cortical activity in essential tremor. Lancet 2001; 357: 519–23.

Helmchen C, Hagenow A, Miesner J, Sprenger A, Rambold H, Wenzelburger R, et al. Eye movement abnormalities in essential tremor may indicate cerebellar dysfunction. Brain 2003; 126: 1319–32.

Hirai T, Miyazaki M, Nakajima H, Shibazaki T, Ohye C. The correlation between tremor characteristics and the predicted volume of effective lesions in stereotaxic nucleus ventralis intermedius thalamotomy. Brain 1983; 106: 1001–18.

Holmes CJ, Hoge R, Collins L, Woods R, Toga AW, Evans AC. Enhancement of MR images using registration for signal averaging. J Comput Assist Tomogr 1998; 22: 324–33.

Hua SE, Lenz FA. Posture-related oscillations in human cerebellar thalamus in essential tremor are enabled by voluntary motor circuits. J Neurophysiol 2005; 93: 117–27.

Indefrey P, Levelt WJM. The neural correlates of language production. In: The new cognitive neurosciences; 2nd ed. Cambridge, MA: MIT Press; 2000. p. 845–65.

Jenkins IH, Bain PG, Colebatch JG, Thompson PD, Findley LJ, Frackowiak RSJ, et al. A positron emission tomography study of essential tremor: evidence for overactivity of cerebellar connections. Ann Neurol 1993; 34: 82–90.

Kahan J, Mancini L, Urner M, Friston K, Hariz M, Holl E, et al. Therapeutic subthalamic nucleus deep brain stimulation reverses cortico-thalamic coupling during voluntary movements in parkinson's disease. PLoS One 2012; 7: e50270.

Kahan J, Urner M, Moran R, Flandin G, Marreiros A, Mancini L, et al. Resting state functional MRI in Parkinson's disease: the impact of deep brain stimulation on "effective" connectivity. Brain 2014; 137: 1130–44.

Kalbe E, Voges J, Weber T, Haarer M, Baudrexel S, Klein JC, et al. Frontal FDG-PET activity correlates with cognitive outcome after STN-DBS in Parkinson disease. Neurology 2009; 72: 42–49.

Kerssens C, Hamann S, Peltier S, Hu XP, Byas-Smith MG, Sebel PS. Attenuated brain response to auditory word stimulation with sevoflurane: a functional magnetic resonance imaging study in humans. Anesthesiology 2005; 103: 11–19.

Kim JP, Min H-K, Knight EJ, Duffy PS, Abulseoud OA, Marsh MP, et al. Centromedian-parafascicular deep brain stimulation induces differential functional inhibition of the motor, associative, and limbic circuits in large animals. Biol Psych 2013; 74: 917–26.

Klein JC, Barbe MT, Seifried C, Baudrexel S, Runge M, Maarouf M, et al. The tremor network targeted by successful VIM deep brain stimulation in humans. Neurology 2012; 78: 787–95.

Knight EJ, Testini P, Min H-K, Gibson WS, Gorny KR, Favazza CP, et al. Motor and nonmotor circuitry activation induced by subthalamic nucleus deep brain stimulation in patients with parkinson disease: intraoperative functional magnetic resonance imaging for deep brain stimulation. Mayo Clin Proc 2015; 90: 773–85.

Kronenbuerger M, Konczak J, Ziegler W, Buderath P, Frank B, Coenen VA, et al. Balance and motor speech impairment in essential tremor. Cerebellum 2009; 8: 389–98.

Kultas-Ilinsky K, Ilinsky IA. Fine structure of the ventral lateral nucleus (VL) of the macaca mulatta thalamus: cell types and synaptology. J Comp Neurol 1991; 314: 319–49.

Kuo SH, Erickson-Davis C, Gillman A, Faust PL, Vonsattel JP, Louis ED. Increased number of heterotopic Purkinje cells in essential tremor. J Neurol Neurosurg Psych 2011; 82: 1038–40.

Lagrange E, Krack P, Moro E, Ardouin C, Van Blercom N, Chabardes S, et al. Bilateral subthalamic nucleus stimulation improves health-related quality of life in PD. Neurology 2002; 59: 1976–8.

Llinás R, Yarom Y. Properties and distribution of ionic conductances generating electroresponsiveness of mammalian inferior olivary neurones in vitro. J Physiol 1981; 315: 569–84.

Llinás R, Yarom Y. Oscillatory properties of guinea-pig inferior olivary neurones and their pharmacological modulation: an in vitro study. J Physiol 1986; 376: 163–82.

Louis ED, Faust PL, Ma KJ, Yu M, Cortes E, Vonsattel JP. Torpedoes in the cerebellar vermis in essential tremor cases vs. controls. Cerebellum 2011; 10: 812–19.

Louis ED, Faust PL, Vonsattel J-PG, Honig LS, Rajput A, Robinson CA, et al. Neuropathological changes in essential tremor: 33 cases compared with 21 controls. Brain 2007; 130: 3297–307.

Louis ED, Shungu DC, Chan S, Mao X, Jurewicz EC, Watner D. Metabolic abnormality in the cerebellum in patients with essential tremor: a proton magnetic resonance spectroscopic imaging study. Neurosci Lett 2002; 333: 17–20.

Louis ED, Vonsattel JP, Honig LS, Lawton A, Moskowitz C, Ford B, Frucht S. Essential tremor associated with pathologic changes in the cerebellum. Arch Neurol 2006; 63: 1189–93.

Louis ED. Essential tremor. Lancet Neurol 2005; 4: 100–10.

Marsden JF, Ashby P, Limousin-Dowsey P, Rothwell JC, Brown P. Coherence between cerebellar thalamus, cortex and muscle in man. Brain 2000; 123: 1459–70.

Matta BF, Heath KJ, Tipping K, Summors AC. Direct cerebral vasodilatory effects of sevoflurane and isoflurane. Anesthesiology 1999; 91: 677–80.

McAuley JH, Marsden CD. Physiological and pathological tremors and rhythmic central motor control. Brain 2000; 123: 1545–67.

McIntyre CC, Grill WM, Sherman DL, Thakor NV. Cellular effects of deep brain stimulation: model-based analysis of activation and inhibition. J Neurophysiol 2004a; 91: 1457–69.

McIntyre CC, Savasta M, Kerkerian-Le Goff L, Vitek JL. Uncovering the mechanism(s) of action of deep brain stimulation: activation, inhibition, or both. Clin Neurophysiol 2004b; 115: 1239–48.

McPherson RW, Traystman RJ. Fentanyl and cerebral vascular responsivity in dogs. Anesthesiology 1984; 60: 180–6.

Neely KA, Kurani AS, Shukla P, Planetta PJ, Wagle Shukla A, Goldman JG, et al. Functional brain activity relates to 0-3 and 3-8 Hz force oscillations in essential tremor. Cereb Cortex 2015; 25: 4191–202.

Nicoletti G, Manners D, Novellino F, Condino F, Malucelli E, Barbiroli B, et al. Diffusion tensor MRI changes in cerebellar structures of patients with familial essential tremor. Neurology 2010; 74: 988–94.

Nii Y, Uematsu S, Lesser RP, Gordon B. Does the central sulcus divide motor and sensory functions? Cortical mapping of human hand areas as revealed by electrical stimulation through subdural grid electrodes. Neurology 1996; 46: 360–7.

Paek SB, Min H-K, Kim I, Knight EJ, Baek JJ, Bieber AJ, et al. Frequency-dependent functional neuromodulatory effects on the motor network by ventral lateral thalamic deep brain stimulation in swine. NeuroImage 2015; 105: 181–8.

Pagan FL, Butman JA, Dambrosia JM, Hallett M. Evaluation of essential tremor with multi-voxel magnetic resonance spectroscopy. Neurology 2003; 60: 1344–7.

Paris-Robidas S, Brochu E, Sintes M, Emond V, Bousquet M, Vandal M, et al. Defective dentate nucleus GABA receptors in essential tremor. Brain 2012; 135: 105–16.

Pascual-Leone A, Valls Solé J, Toro C, Wassermann EM, Hallett M. Resetting of essential tremor and postural tremor in Parkinson's disease with transcranial magnetic stimulation. Muscle Nerve 1994; 17: 800–7.

Pedrosa DJ, Auth M, Pauls KA, Runge M, Maarouf M, Fink GR, et al. Verbal fluency in essential tremor patients: the effects of deep brain stimulation. Brain Stimul 2014; 7: 359–64.

Penfield W, Boldrey E. Somatic motor and sensory representation in the cerebral cortex of man as studied by electrical stimulation. Brain 1937; 60: 389–443.

Perlmutter JS, Mink JW, Bastian AJ, Zackowski K, Hershey T, Miyawaki E, et al. Blood flow responses to deep brain stimulation of thalamus. Neurology 2002; 58: 1388–94.

Pinto AD, Lang AE, Chen R. The cerebellothalamocortical pathway in essential tremor. Neurology 2003; 60: 1985–7.

Plourde G, Belin P, Chartrand D, Fiset P, Backman SB, Xie G, et al. Cortical processing of complex auditory stimuli during alterations of consciousness with the general anesthetic propofol. Anesthesiology 2006; 104: 448–57.

Popa T, Russo M, Vidailhet M, Roze E, Lehericy S, Bonnet C, et al. Cerebellar rTMS stimulation may induce prolonged clinical benefits in essential tremor, and subjacent changes in functional connectivity: an open label trial. Brain Stim 2013; 6: 175–9.

Quattrone A, Cerasa A, Messina D, Nicoletti G, Hagberg GE, Lemieux L, et al. Essential head tremor is associated with cerebellar vermis atrophy: a volumetric and voxel-based morphometry MR imaging study. Am J Neuroradiol 2008; 29: 1692–7.

Raethjen J, Deuschl G. The oscillating central network of essential tremor. Clin Neurophysiol 2012; 123: 61–4.

Raethjen J, Govindan RB, Kopper F, Muthuraman M, Deuschl G. Cortical involvement in the generation of essential tremor. J Neurophysiol 2007; 97: 3219–28.

Rehncrona S, Johnels B, Widner H, Törnqvist AL, Hariz M, Sydow O. Long term efficacy of thalamic deep brain stimulation for tremor: double blind assessments. Mov Disord 2003; 18: 163–70.

Ruskin K, Rosenbaum S, Ij R. Fundamentals of neuroanesthesia: a physiologic approach to clinical practice. Oxford: Oxford Press; 2013.

Saad ZS, Glen DR, Chen G, Beauchamp MS, Desai R, Cox RW. A new method for improving functional-to-structural MRI alignment using local Pearson correlation. NeuroImage 2009; 44: 839–48.

Safo Y, Young ML, Smith DS, Greenberg J, Carlsson C, Reivich M, et al. Effects of fentanyl on local cerebral blood flow in the rat. Acta Anaesthesiol Scand 1985; 29: 594–8.

Schaltenbrand G, Wahren W. Atlas for stereotaxy of the human brain: architectonic organisation of the thalamic nuclei by rolf hassler. Stuttgart: Georg Thieme Publishers; 1977.

Schell GR, Strick PL. The origin of thalamic inputs to the arcuate premotor and supplementary motor areas. J Neurosci 1984; 4: 539–60.

Schelter B, Timmer J, Eichler M. Assessing the strength of directed influences among neural signals using renormalized partial directed coherence. J Neurosci Methods 2009; 179: 121–30.

Schnitzler A, Münks C, Butz M, Timmermann L, Gross J. Synchronized brain network associated with essential tremor as revealed by magnetoencephalography. Mov Disord 2009; 24: 1629–35.

Schroeder U, Kuehler A, Lange KW, Haslinger B, Tronnier VM, Krause M, et al. Subthalamic nucleus stimulation affects a fronto-temporal network: a PET study. Ann Neurol 2003; 54: 445–50.

Shill HA, Adler CH, Sabbagh MN, Connor DJ, Caviness JN, Hentz JG, et al. Pathologic findings in prospectively ascertained essential tremor subjects. Neurology 2008; 70: 1452–5.

Stefurak T, Mikulis D, Mayberg H, Lang AE, Hevenor S, Pahapill P, et al. Deep brain stimulation for Parkinson's disease dissociates mood and motor circuits: a functional MRI case study. Mov Disord 2003; 18: 1508–16.

Stolze H, Petersen G, Raethjen J, Wenzelburger R, Deuschl G. The gait disorder of advanced essential tremor. Brain 2001; 124: 2278–86.

Sydow O, Thobois S, Alesch F, Speelman JD. Multicentre European study of thalamic stimulation in essential tremor: a six year follow-up. J Neurol Neurosurg Psych 2003; 74: 1387–91.

Vidailhet M, Vercueil L, Houeto J-L, Krystkowiak P, Benabid AL, Cornu P, et al. Bilateral deep-brain stimulation of the globus pallidus in primary generalized dystonia. N Engl J Med 2005; 352: 459–67.

Welsh JP, Lang EJ, Suglhara I, Llinás R. Dynamic organization of motor control within the olivocerebellar system. Nature 1995; 374: 453–7.

Wills AJ, Jenkins IH, Thompson PD, Findley LJ, Brooks DJ. Red nuclear and cerebellar but no olivary activation associated with essential tremor: a positron emission tomoraphic study. Ann Neurol 1994; 36: 636–42.

Wills AJ, Jenkins LH, Thompson PD, Findley LJ, Brooks DJ. A positron emission tomography study of cerebral activation associated with essential and writing tremor. Arch Neurol 1995; 52: 299–305.

Windels F, Bruet N, Poupard A, Feuerstein C, Bertrand A, Savasta M. Influence of the frequency parameter on extracellular glutamate and γ aminobutyric acid in substantia nigra and globus pallidus during electrical stimulation of subthalamic nucleus in rats. J Neurosci Res 2003; 72: 259–67.

Windels F, Bruet N, Poupard A, Urbain N, Chouvet G, Feuerstein C, et al. Effects of high frequency stimulation of subthalamic nucleus on extracellular glutamate and GABA in substantia nigra and globus pallidus in the normal rat. Eur J Neurosci 2000; 12: 4141–6.

Yu M, Ma K, Faust PL, Honig LS, Cortes E, Vonsattel JPG, et al. Increased number of Purkinje cell dendritic swellings in essential tremor. Eur J Neurol 2012; 19: 625–30.